INORGANIC CHEMISTRY
FRONTIERS

RESEARCH ARTICLE

View Article Online
View Journal | View Issue

Cite this: *Inorg. Chem. Front.*, 2024, **11**, 1742

Straightforward construction of a rare-earth diphosphanato complex from white phosphorus: synthesis and reactivity†

Fangjun Zhang,[a] Iker del Rosal,[b] Keyu Han,[a] Jie Zhang,*[a] Laurent Maron*[b] and Xigeng Zhou*[a]

The direct construction of functionalized diphosphine ligands from P_4 is a highly valuable but challenging transformation. In this work, a simple method has been developed for the direct formation of an amido-functionalized diphosphanato ligand from a silyl-bridged amido/methylene yttrium complex and white phosphorus. The resulting amido-functionalized diphosphanato yttrium complex **2** has proved to be a useful intermediate for further diversification of the diphosphine ligand through the metal template procedure, for which no evident limitations are enforced by initially present substituents and ancillary ligands, and some unprecedented reactivity patterns of the RPPR unit are revealed. The results described here demonstrate that appending a strongly coordinative substituent to the alkyl ligand together with a coordination to rare earth ions is an efficient strategy for controlling the cleavage modes of P_4 during alkylation and the reactivity of the resulting diphosphanato complex.

Received 28th December 2023,
Accepted 16th February 2024

DOI: 10.1039/d3qi02680a

rsc.li/frontiers-inorganic

Introduction

Diphosphine-based ligands play an important role in catalysis, coordination and organometallic chemistry.[1–3] To tune their properties for potential applications and improve the overall synthetic efficiency, significant effort continues to be devoted to the development of new approaches for their synthesis and new diphosphine-based structures.[4–6] Among these approaches, the introduction of one or more heteroatoms (*e.g.* O, N, S, Se, Si, and F) into diphosphine backbones is especially attractive, as the presence of heteroatoms will have a much greater influence on the coordination modes and donor ability than the variation of organic substituents at the P atoms, and thus offers new opportunities for controlling the reactivity trends, catalytic behaviour and physical properties of metal complexes.[7–12] For example, the pendant amines on diphosphine ligands facilitate the binding and heterolytic cleavage of H_2 or serve as proton and hydride relays for metal-mediated hydrogen transfers.[9c,d]

Traditionally, multifunctionalized diphosphine ligands are prefabricated by stepwise processes starting from PCl_3 or its equivalents before application in organic and organometallic syntheses. Alternatively, in a few cases they can be generated *in situ* by the reaction of a metal phosphinido or phosphinidene complex intermediate (Scheme 1A).[13] Obviously, these synthetic approaches to metal complexes containing polyfunctional diphosphine ligands often require expensive and/or toxic reagents and generate a large amount of waste, further compounded by limitations of substituent scope due to difficulties in preparing related P-based reactant precursors. If white phosphorus (P_4) could be directly used in the construction of polyfunctional diphosphine ligands, it would provide a simpler, more environmentally benign and higher atom-economical process compared to the use of classical methods involving pollutants, such as PCl_3, as starting materials. Although a great deal of effort has been devoted to the activation of P_4 over the last four decades, reactions that can form diphosphine skeletons either as free species or as complexed ligands remain scarce.[6,14–17] In fact, there are currently no generally satisfactory routes to the formation of polyfunctional diphosphine moieties from P_4 without the formation of byproducts. The functionalization of P_4 using alkyl/aryl metal complexes is relatively uncontrollable and tends to form monophosphanes or partly P-alkylated (arylated) polyphosphorus species (Scheme 1B).[16,18,19] The difficulty of forming the diphosphanato or diphosphenyl complexes may reflect the challenge of controlling the cleavage pattern of P_4 during alkylation/arylation, requiring a larger energy input for the simultaneous clea-

[a]*Department of Chemistry, Fudan University, No. 2005, Songhu Road, Shanghai 200438, China. E-mail: zhangjie@fudan.edu.cn, xgzhou@fudan.edu.cn*
[b]*LPCNO, CNRS, and INSA, Université Paul Sabatier, 135 Avenue de Rangueil, Toulouse 31077, France. E-mail: laurent.maron@irsamc.ups-tlse.fr*

†Electronic supplementary information (ESI) available. CCDC 1879573 (**1**), 1879574 (**2**), 1879577 (**2·THF**), 1879583 (**3**), 1879582 (**4**), 1879576 (**5**), 1879581 (**6**), 1879575 (**7**·0.5C_6H_{14}), 1879580 (**8**), 1879579 (**9**), and 1879578 (**10**). For ESI and crystallographic data in CIF or other electronic format see DOI: https://doi.org/10.1039/d3qi02680a

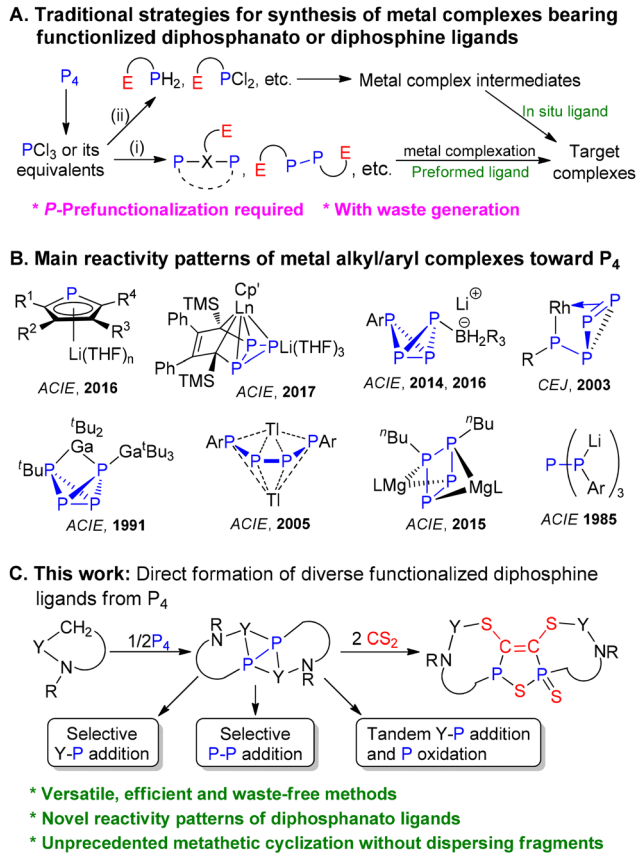

Scheme 1 Synthetic strategies to access functionalized diphosphanato and diphosphine metal complexes and main reactivity patterns of metal alkyl/aryl complexes toward P_4.

vage of four P–P bonds compared with that for the relatively small number of P–P bonds in the formation of $[P_4R_m]^{n-}$ (m = 1–3; n = 0–4; R = alkyl, aryl) moieties.

On the other hand, although metal-based reductive cleavage of P_4 to give a diphosphorus ligand is a well-established process, the exploration of the resulting P_2 fragment as a synthon for diphosphines remains limited.[20] Pioneering works reported by West, Bertrand, and Cummins *et al.* showed that the activation of P_4 by disilenes, carbenes or photochemical alkylation could lead to the formation of the corresponding silylene-, alkylidenyl- and alkyl-substituted diphosphanes, respectively, and these findings open new avenues for the generation of reactive intermediates in P_2 chemistry.[4a,e,5b,6]

Metal diphosphanato complexes could be considered as attractive intermediates for the synthesis of a variety of neutral or anionic diphosphine ligands as evidenced by their participation in the formation of carbon–phosphorus and heteroatom–phosphorus bonds.[21,22] However, this class of compounds are still rare due to challenges in their synthesis.[23] Given the pronounced ability of rare earth metals to influence the reactivity of small molecule substrates and high activity of lanthanide–alkyl bonds,[24,25] we reasoned that the obstacles encountered in the direct conversion of P_4 to dialkyldiphosphanato complexes *via* reductive insertion processes might be overcome by appending the strong chelating coordination moiety to the alkyl ligand together with a coordination to lanthanide ions, because this not only offers a sterically forced preferred orientation of the nucleophilic attack at P_4 in an expected position for regioselective cleavage of P–P bonds, but also may inhibit the alkyl migration between P atoms (Scheme 1C). Here, we report a simple method for the direct and highly atom-economical construction and late-stage diversification of amido-functionalized diphosphanato ligands from white phosphorus enabled by rare earth metals, for which some unprecedented reactivity patterns of the RPPR moiety toward small molecule substrates are revealed.

Results and discussion

A new silyl-bridged amido/methylene yttrium complex **1** was prepared by the reaction of $Tp^{Me2}YBn_2(THF)$ (Bn = CH_2Ph) with $HN(SiMe_3)_2$. Surprisingly, only a low yield of **1** was obtained when 1 equiv. of $HN(SiMe_3)_2$ was used, and complete transformation of $Tp^{Me2}YBn_2(THF)$ into **1** would require the use of 2 equiv. of $HN(SiMe_3)_2$ (Scheme 2). These results indicate that **1** probably results from amine elimination of intermediate **B** rather than the toluene elimination of **A**, and steric crowding around the metal center might play a more important role than ligand basicity in driving the methyl deprotonation. Complex **1** has been characterized by elemental analysis, ^1H and $^{13}C\{^1H\}$ NMR spectra, and its solid-state structure has also been determined by X-ray diffraction analysis (Fig. S26†).

Treatment of **1** with 0.25 equiv. of P_4 in toluene at ambient temperature afforded the Y–C bond insertion/coupling product **2** in 60% isolated yield (Scheme 2), which represents the first example of the efficient formation of amido-functionalized diphosphanato metal complexes directly from P_4. Complex **2** is readily soluble in THF but sparingly soluble in toluene. The ^{31}P NMR spectrum of **2** displayed a triplet peak at δ = 97.10 ppm ($^1J_{YP}$ = 30 Hz), indicating that its binuclear structure is symmetric. Consistent with this, only one set of signals attributable to the Tp^{Me2} ligand was observed in the ^1H and $^{13}C\{^1H\}$ NMR spectra of **2**. Crystallization of **2** in THF gave the THF adduct **2·THF**. Significantly, the THF coordination triggers the difunctionalized diphosphanato ligand to isomerize from *trans* to *cis* (Fig. 1). Furthermore, in contrast to **2**, **2·THF**

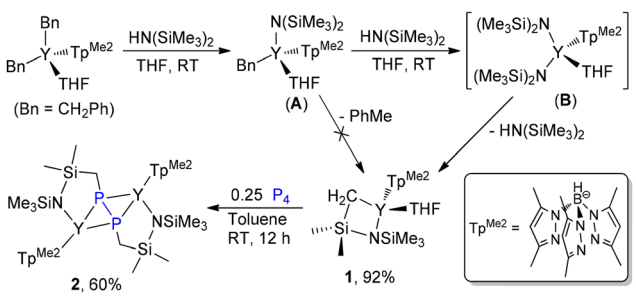

Scheme 2 Synthesis of 1,2-dialkyldiphosphanato yttrium complex **2**.

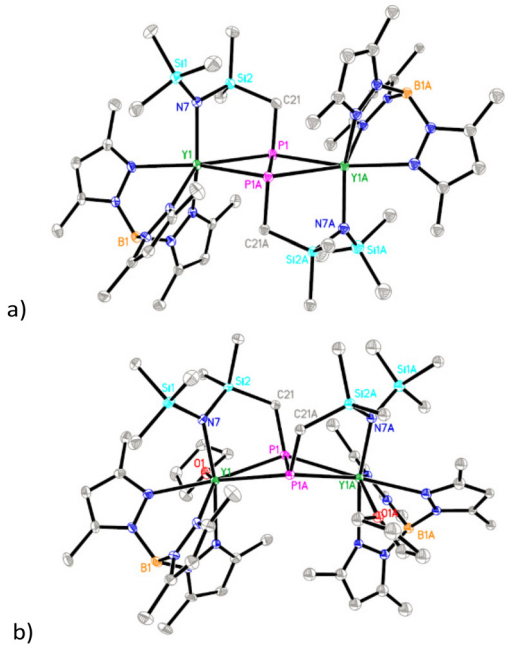

Fig. 1 Molecular structures of **2** (a) and **2·THF** (b) with 30% thermal ellipsoids. All hydrogen atoms are omitted for clarity.

is insoluble in THF. The P–P distance in **2** (2.213(2) Å) is slightly longer than the values observed in $Cp_2NbH(P_2Ph_2)$ (2.136(5) Å) and $Cp_2TaH(P_2Cy_2)$ (2.131(3) Å).[15]

It should be noted that the chelating coordination of the pendant amido moiety might play a key role in determining the formation of **2**. In our previous study,[26] we found that the rare-earth dialkyl complex $Tp^{Me2}LnBn_2(THF)$ reacts with P_4 to yield novel rare-earth norbornane-BnP_7^{4-} and/or chain $Bn_4P_6^{4-}$ complexes, accompanied by the formation of PBn_3,[26b] and the rare-earth monoalkyl complex LYR(THF) (L = *N*,*N*′-2,6-diisopropylphenyl-1,4-diazabutadiene, R = $CH_2C_6H_4NMe_2$-2) reacts with P_4 to give a rare-earth organic *cyclo*-P_4 complex $(LY{\cdot}DMAP)_2[1,2\text{-}R_2\text{-}cyclo\text{-}P_4]$, which further transforms into other polyphosphorus species through alkyl migration.[26c] These results demonstrate that appending a strongly coordinative amino substituent to the alkyl group, together with a coordination to Y^{3+} ions, surely offers a good stabilizing environment for 1,2-dialkyldiphosphanato dianion species.

CS_2 is a cheap and manageable feedstock for the synthesis of sulfur-containing molecules, and the development of new reactivity patterns of CS_2 and new methods for its activation under mild conditions is attracting scientific and industrial interest, including its use as a model for CO_2 and its implication in catalytic degradation of CS_2 pollutants.[27,28] Despite tremendous advances in fragmented coupling reactions involving CS_2, there is no report on the combined reorganization/cyclization of CS_2 with other organic functional groups.[28,29] Contrary to the metal complexes bearing other phosphorus-based ligands (*e.g.* phosphinidene and phosphinido),[13b,30] treatment of **2** with two equiv. of CS_2 in THF at room temperature led to the formation of the highly reorganized 2-sulfido-

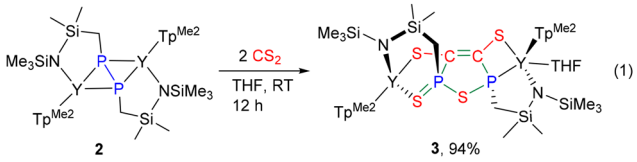

Scheme 3 Reaction of 1,2-dialkyldiphosphanato yttrium complex **2** with CS_2.

2,5-dihydro-1,2,5-thiadiphosphole-3,4-dithiolate dianion ligand that bridges the two yttrium atoms in a non-symmetric fashion (Scheme 3). Noticeably, the reaction works almost exclusively for the formation of **3**. Our attempts to use 1 equiv. of CS_2 for the isolation of the reaction intermediates afforded **3** with the recovery of significant quantities of the starting material **2**, which was also detected from ^{31}P NMR spectra at the end of the reaction. The X-ray structure of **3** (Fig. 2) reveals that the resulting thiadiphosphole ring was coplanar. The C41–C42 distance (1.332(6) Å) is a normal C=C double bond length. The P1–S3 and P2–S3 distances (2.157(2) and 2.100(2) Å, respectively) exhibit typical P–S single bond characteristics, whereas the P2–S4 distance (1.999(2) Å) falls in the range of the P=S double bond lengths (1.949–2.09 Å).[31] The Y2–S4 distance (2.805(2) Å) is longer than the Y2–S2 one (2.727(2) Å). The ^{31}P NMR spectrum of **3** shows two characteristic signals at δ = 92.43 ppm (q, P1, $^1J_{YP}$ = 17.6 Hz) and 47.88 ppm (s, P2). The ^{13}C $\{^1H\}$ NMR spectrum of **3** displays two sets of peaks at δ = 152.68 ppm (dd, $^1J_{PC}$ = 3.21 Hz, $^2J_{YC}$ = 1.56 Hz) and 152.21 ppm (d, $^1J_{PC}$ = 1.99 Hz), attributable to the resonances of the carbon atoms of the thiadiphosphole ring.

The great success of alkene metathesis has stimulated research activity aimed at mapping the analogous reactivity modes of unsaturated carbon–heteroatom functionalities.[32,33] However, CS_2 metathesis reactions remain little explored. In contrast to the classical metatheses, the formation of **3** is not accompanied by the loss of any fragments. This finding provides a new probe for designing convergent metatheses that allow the simultaneous cleavage of multiple different chemical bonds and sequential incorporation of all fragments into a single organic architecture, without any fragment dispersion.

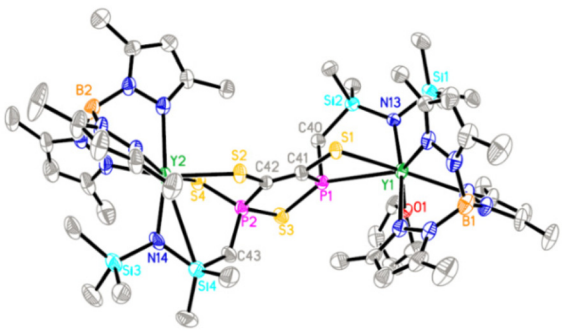

Fig. 2 Molecular structure of **3** with 30% thermal ellipsoids. All hydrogen atoms are omitted for clarity.

To obtain an insight into the driving force for the reaction, the reaction was further investigated by theoretical calculations at the DFT level. The reaction profile appears to be quite complex (Fig. S34, ESI†). The reaction begins by the sequential addition of two CS_2 molecules to the diphosphanato ligand. These electrophilic additions of CS_2 to the phosphorus are kinetically accessible and the height of the barrier is only associated with the binding of the incoming CS_2. This yields complex **D**, which is thermodynamically favorable (22.4 kcal mol^{-1}). From there, one CS_2 moiety can undergo a [2 + 2] addition to the P–P bond that is activated by the two electrophilic additions. This reaction is not assisted by the metal center, explaining that this is the rate determining step. After this migratory insertion, the C–S bond becomes strongly activated and can be easily cleaved to form a P–S–P bridge (complex **F**). The lack of stability of complex **F** allows further reaction. A kinetically accessible intramolecular cyclization transition state has been located, yielding a stable five-membered ring complex **G** (−30.1 kcal mol^{-1}). This complex undergoes a facile metal-assisted intramolecular C–S bond activation, affording the formation of the very stable complex **3** (−77.1 kcal mol^{-1}).

Diphosphorus ligands connected by a single atom have drawn considerable interest due to their complementary properties to wide bite-angle diphosphine ligands in homogeneous catalysis.[34] Interestingly, the reaction of **2** with excess CO (1 atm) at 50 °C afforded the P–P and Y–P bond insertion product **4** (Scheme 4). The resulting carbonyl-bridged diphosphorus anion ligand features an additional degree of electron-delocalization control over the P⋯C⋯O binding sites. In the ^{1}H NMR spectra of **4**, the two sets of signals for the methyl protons of Me_3Si substituents (δ −0.13 and −0.09 ppm) are consistent with the observation that the Y^{3+} ions have two different coordination environments. Moreover, different chemical shifts assigned to the two Tp^{Me2} ligands were observed in its ^{1}H NMR spectrum. The ^{31}P NMR spectrum shows two peaks at δ = 65.01 (d, $^1J_{YP}$ = 136.4 Hz) and −11.89 (d, $^1J_{YP}$ = 120.3 Hz) ppm. X-ray single crystal diffraction analyses of **4** (Fig. 3) clearly demonstrate the insertion of one CO molecule into the P–P bond to form a C–P single bond and a C=P double bond. Complex **4** has a distinctive Y–O(phosphaenolate) distance (2.153(2) Å).

The catalytic carbonylation of organic substrates has become a powerful method in organic synthesis. Despite tremendous advances in this area, this process has mainly focused on late transition metals. Rare earth-mediated CO

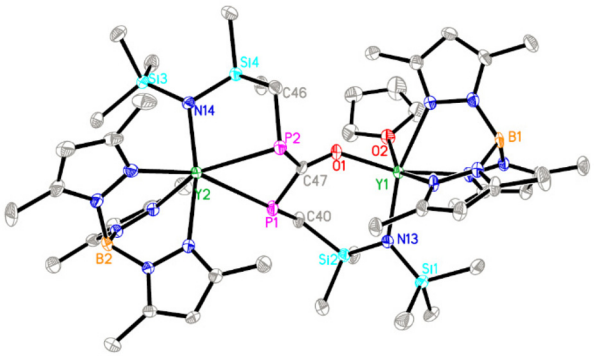

Fig. 3 Molecular structure of **4** with 30% thermal ellipsoids. All hydrogen atoms are omitted for clarity.

insertions have been largely unexplored. This is mainly due to the mismatch in the orbital energy between the hard rare earth ions and the soft carbon monoxide (or acyl) ligand, leading to an unstable acyl complex intermediate having a strong tendency toward dimerization or deoxygenative coupling.[13b,35,36] Therefore, the formation of **4** is somewhat surprising. To explain the unusual reactivity of **2** toward CO, a DFT investigation of a possible reaction mechanism was carried out (see Fig. S35†). It is found that CO insertion into a Y–P bond followed by the migration of another P atom to the resulting acyl carbon is a knetically facile (highest barrier of 13.8 kcal mol^{-1}) and thermodynamically favorable process (−33.9 kcal mol^{-1}). This is quite different from the conventional oxidative-addition followed by CO insertion and sequential reductive-elimination pathways for transition-metal-mediated CO insertion into a single bond of organic substrates.

To validate our proposal of the preferential addition of the Y–P bond over the P–P bond, we carried out the reaction of **2** with PhNCS (Scheme 5). The addition of 2 equiv. of PhNCS to a THF solution of **2** resulted in an immediate color change, yielding a colorless solution, and storing the solution at room temperature for 48 h gave the Y–P bond insertion product **5** as

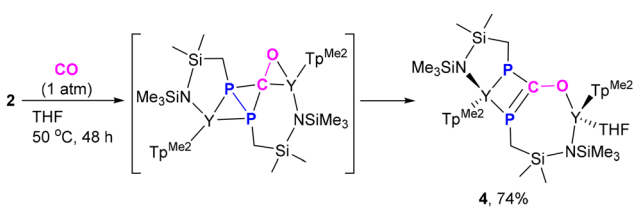

Scheme 4 CO insertion into the P–P and Y–P bonds *via* an unusual Y–P addition and sequential phosphanyl migration pathway.

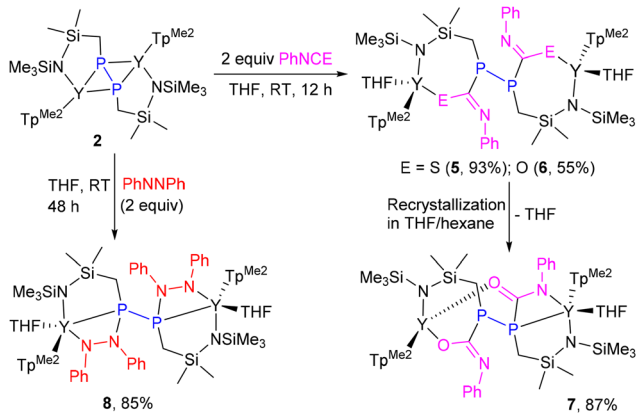

Scheme 5 Insertions of PhNCS, PhNCO and PhN=NPh into the Y–P bond of **2**.

colorless crystals in 93% isolated yield. In contrast to CS_2 and CO, complex **5** did not undergo either isomerization or further reaction with excess PhNCS, even with prolonged heating at 70 °C. Regrettably, the low solubility of **5** precluded the acquisition of its NMR spectra. The same reactivity trend was observed when **2** reacted with 2 equiv. of PhNCO, giving the addition product **6**. Recrystallization of **6** in THF/hexane led to the loss of one coordinated THF, giving compound **7**, in which a different coordination situation of the diphosphine ligand was observed (Scheme 5). In contrast to **5**, compounds **6** and **7** readily dissolve in THF. Notably, the transformation of **6** into **7** occurred slowly under vacuum conditions or exposure to nitrogen gas too. The ^{31}P NMR spectrum of **7** shows two sets of signals at δ −39.64 (dd, J_{PP} = 374, 12.8 Hz) and −26.71 (dm, $^1J_{PP}$ = 374 Hz) ppm, which may be attributed to the free and coordinated P atoms, respectively.[20d] The molecular structures of complexes **5**–**7** clearly indicate the formation of four-substituted diphosphine moieties (Fig. S28–S30†).

The ^{31}P NMR monitoring data indicate that the reaction of **2** with azobenzene is much slower than those with CS_2 and PhNCO, which likely resulted from the larger steric hindrance and the non-polarity effect of azobenzene.[37,38] Compound **8** was sparingly soluble in THF-d_8, enabling the acquisition of ^{1}H NMR and ^{31}P NMR data, but preventing characterization by ^{13}C {^{1}H} NMR spectra. The ^{31}P NMR spectrum displays only a singlet at δ = 50.66 ppm, revealing that **8** is a symmetric structure as confirmed by X-ray crystallography (Fig. S31 in the ESI†).

The reaction of **2** with 0.5 equiv. of S_8 in THF at room temperature gave the diphosphinodithioate complex **9** in 94% yield. Chalcogenylation is of great significance in adjusting the complexation ability and catalytic behaviour of diphosphines or in their potential utilization as synthetic intermediates.[39a,40] Despite a large number of structural variants, such a substitution pattern for diphosphorus-containing species is still unknown due to the absence of suitable synthetic methods. Although the chemistry of phosphine sulfide and selenide ligands has been extensively investigated, the complexes of diphosphoranes containing P–P bonds are primarily limited to diphosphane mono- and di-sulfides/selenides.[39b,40] The polychalcogenylations of either neutral or anionic P–P units with elemental sulfur (selenium) are typically accompanied by the P–P cleavage.[21] To obtain a good insight into the formation process of **9**, we firstly attempted the reaction of **2** with 0.25 equiv. of S_8, but it generated a mixture of **9** and several unidentified products. Furthermore, the reaction of **2** with Se, which is known to have relatively modest reactivity compared with S_8, was examined. **2** reacted with 3 equiv. of Se to yield the diphosphine triselenide complex **10** in 83% yield (Scheme 6). Despite several attempts, we were unable to gain the structural information of the product from a similar reaction of **2** with 4 equiv. of Se, owing to its low solubility even in polar organic solvents such as THF. The formation of **9** and **10** could be interpreted as a sulfur/selenium insertion into each Y–P bond of **2**, followed by oxidative chalcogenylation of phosphorus. This further demonstrates that the reactivity of diphosphanato ligands toward small molecules may be adjusted by

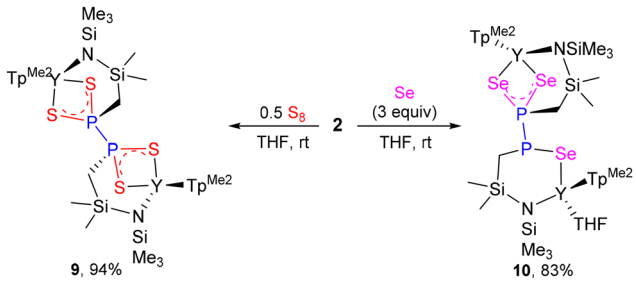

Scheme 6 Oxidative chalcogenylation of **2** with S_8 and Se.

complexation of Y^{3+} ions. Complexes **9** and **10** were fully characterized; this information, including their single-crystal X-ray structures, can be found in the ESI (Fig. S32 and S33†).

Experimental

General procedures

All manipulations involving air- and moisture-sensitive compounds were carried out with rigorous exclusion of air and water, using standard Schlenk techniques or a Vigor glovebox under an atmosphere of dinitrogen. THF, toluene and hexane were purified using an Mbraun SPS-800 solvent purification system, dried over fresh Na chips and stored in the glovebox. C_6D_6 and THF-d_8 were obtained from Cambridge Isotope and dried over Na/K alloy prior to use. (Tp^{Me2})YBn_2(THF) was prepared according to the literature procedure.[41] $HN[Si(CH_3)_3]_2$, CS_2, PhNCS and PhNCO were purchased from J&K and dried with 4 Å sieves. Other commercially available reagents were purchased and used without purification. P_4 was prepared by sublimation of red phosphorus at 450 °C in a quartz tube under vacuum conditions and stored in the refrigerator of the glovebox. Organometallic samples for NMR spectroscopic measurements were prepared in the glovebox using J. Young valve NMR tubes. ^{1}H NMR, ^{13}C NMR and ^{31}P NMR spectra were recorded using a Bruker Avance 400 MHz spectrometer (FT, 400 MHz for ^{1}H; 100 MHz for ^{13}C; and 161 MHz for ^{31}P) at room temperature. Chemical shifts for ^{1}H and ^{13}C NMR were quoted in ppm referenced to the residual resonance of the deuterated solvents. H_3PO_4 (85%) sealed in a capillary was used as an external standard in ^{31}P NMR analysis. Elemental analyses for C, H and N were carried out using a Vario EL III elemental analyzer. *The resonances of the B–H bond in the Tp^{Me2} ligand are too broad to be observed in their ^{1}H NMR spectra.* **Caution:** P_4 is light-sensitive and highly flammable upon exposure to air. It should be handled carefully.

Synthesis of 1

A THF solution of $HN[Si(CH_3)_3]_2$ (3.22 g, 20.0 mmol) was added slowly to a stirred THF solution (50 mL) of $Tp^{Me2}YBn_2$(THF) (6.40 g, 10.0 mmol) at room temperature. After stirring for 8 hours, all volatiles were removed under vacuum. The residue was washed twice with *n*-hexane (10 mL ×

2) and dried under vacuum to give 1 as a white powder (5.67 g, 92% yield). Recrystallization of the white powder in a mixed solvent of THF and *n*-hexane afforded colorless crystals of 1 suitable for X-ray diffraction analysis. ^{1}H NMR (400 MHz, C_6D_6, 25 °C): δ (ppm) 5.56 (s, 3H, 4-*H*-Tp^{Me2}), 3.56 (m, 4H, *THF*), 2.50 (s, 9H, 3-CH_3-Tp^{Me2}), 2.10 (s, 9H, 5-CH_3-Tp^{Me2}), 1.14 (m, 4H, *THF*), 0.79 (s, 6H, Si(CH_3)$_2$), 0.33 (s, 9H, Si(CH_3)$_3$), 0.13 (d, $^2J_{YH}$ = 1.6 Hz, 2H, SiCH_2Y); ^{13}C{^{1}H} NMR (100 MHz, C_6D_6, 25 °C): δ (ppm) 150.13 (Tp^{Me2}), 145.49 (Tp^{Me2}), 105.91 (4-*C*-Tp^{Me2}), 71.27 (*THF*), 26.90 (d, $^1J_{YC}$ = 30.81 Hz, SiCH$_2$Y), 25.29 (*THF*), 14.73 (*C*H$_3$-Tp^{Me2}), 13.07 (*C*H$_3$-Tp^{Me2}), 8.33 (s, Si(*C*H$_3$)$_2$), 8.32 (s, Si(*C*H$_3$)$_2$), 5.74 (Si(*C*H$_3$)$_3$). Elemental analysis: calcd (%) for $C_{25}H_{47}N_7BOSi_2Y$: C, 48.62; H, 7.67; N, 15.88. Found: C, 48.04; H, 7.74; N, 16.17.

Synthesis and characterization of the diphosphanato yttrium complex 2 and 2·THF

P_4 (31.0 mg, 0.25 mmol) was added to a stirred toluene solution (2 mL) of **1** (617 mg, 1.0 mmol) at ambient temperature. The color of the reaction mixture gradually changed from light yellow to reddish brown. After half an hour, a pale solid began to precipitate out. The mixture was continuously stirred overnight, and the precipitate was filtered under reduced pressure, washed with 2 mL of *n*-hexane and dried under vacuum to give **2** as a pale yellow powder (342 mg, 60% yield). Yellow crystals of **2** suitable for X-ray single crystal diffraction analysis were obtained by evaporation of the solvent from the solution of **2** in a 30 : 1 mixture of toluene and THF. ^{1}H NMR (400 MHz, THF-d_8, 25 °C): δ (ppm) 5.76 (s, 2H, 4-*H*-Tp^{Me2}), 5.74 (s, 2H, 4-*H*-Tp^{Me2}), 5.25 (s, 2H, 4-*H*-Tp^{Me2}), 2.67 (s, 6H, CH_3-Tp^{Me2}), 2.59 (s, 6H, CH_3-Tp^{Me2}), 2.38–2.33 (m, 24H, CH_3-Tp^{Me2}), 1.29 (s, 4H, SiCH_2P), 0.27 (s, 12H, Si(CH_3)$_2$), 0.15 (s, 18H, Si(CH_3)$_3$); ^{13}C{^{1}H} NMR (100 MHz, THF-d_8, 25 °C): δ (ppm) 152.66 (Tp^{Me2}), 151.79 (Tp^{Me2}), 150.55 (Tp^{Me2}), 145.46 (Tp^{Me2}), 145.35 (Tp^{Me2}), 144.63 (Tp^{Me2}), 106.80 (4-*C*-Tp^{Me2}), 106.20 (4-*C*-Tp^{Me2}), 19.22 (*C*H$_3$-Tp^{Me2}), 15.65 (*C*H$_3$-Tp^{Me2}), 14.67 (m, Si*C*H$_2$P), 13.31 (*C*H$_3$-Tp^{Me2}), 13.18 (*C*H$_3$-Tp^{Me2}), 13.06 (*C*H$_3$-Tp^{Me2}), 8.43 (Si(*C*H$_3$)$_2$), 8.15 (Si(*C*H$_3$)$_2$), 6.15 (Si(*C*H$_3$)$_3$); ^{31}P NMR (161 MHz, THF-d_8, 25 °C): δ (ppm) −97.10 (t, $^1J_{YP}$ = 30 Hz). Elemental analysis: calcd (%) for $C_{42}H_{78}N_{14}B_2Si_4P_2Y_2$: C, 43.76; H, 6.82; N, 17.00. Found: C, 42.86; H, 6.69; N, 17.33. It is noted that recrystallization of **2** in THF afforded **2·THF** as yellow crystals. Elemental analysis: calcd (%) for $C_{50}H_{94}N_{14}B_2O_2Si_4P_2Y_2$: C, 46.30; H, 7.30; N, 15.12. Found: C, 45.66; H, 7.14; N, 15.37. However, the difficulty in redissolving the isolated crystals of **2·THF** prevented its characterization by NMR spectroscopy.

Synthesis of 3

A cooled THF solution (5 mL) of CS_2 (30.3 mg, 0.40 mmol) was added slowly to a stirred THF solution (10 mL) of **2** (230 mg, 0.20 mmol) at ambient temperature. The color of the mixture gradually changed from yellow to reddish brown. After stirring for 1 hour, the solvent was removed under vacuum and the residue was washed twice with *n*-hexane (10 mL × 2) and dried under vacuum to give **3** as a yellow powder (260 mg, 94% yield). Crystals suitable for X-ray analysis were obtained by recrystallization of 3 in toluene. ^{1}H NMR (400 MHz, THF-d_8, 25 °C): δ (ppm) 5.82 (s, 1H, 4-*H*-Tp^{Me2}), 5.81 (s, 1H, 4-*H*-Tp^{Me2}), 5.79 (s, 1H, 4-*H*-Tp^{Me2}), 5.76 (s, 1H, 4-*H*-Tp^{Me2}), 5.68 (s, 1H, 4-*H*-Tp^{Me2}), 5.57 (s, 1H, 4-*H*-Tp^{Me2}), 3.62 (m, *THF*), 2.65 (s, 3H, CH_3-Tp^{Me2}), 2.51 (s, 3H, CH_3-Tp^{Me2}), 2.47 (s, 3H, CH_3-Tp^{Me2}), 2.41–2.40 (m, 18H, CH_3-Tp^{Me2}), 2.37 (s, 3H, CH_3-Tp^{Me2}), 2.28 (s, 3H, CH_3-Tp^{Me2}), 2.22 (s, 3H, CH_3-Tp^{Me2}), 1.94–1.81 (m, 4H, SiCH_2P), 1.77 (m, *THF*), 0.48 (s, 3H, Si(CH_3)$_2$), 0.45 (s, 3H, Si(CH_3)$_2$), 0.30 (s, 3H, Si(CH_3)$_2$), 0.24 (s, 3H, Si(CH_3)$_2$), 0.00 (s, 9H, Si(CH_3)$_3$), −0.50 (s, 9H, Si(CH_3)$_3$); ^{13}C{^{1}H} NMR (100 MHz, THF-d_8, 25 °C): δ (ppm) 152.67 (q, $^1J_{PC}$ = 3.21 Hz, $^2J_{YC}$ = 1.56 Hz, S*C*PS), 152.38 (Tp^{Me2}), 152.22 (d, $^1J_{PC}$ = 1.99 Hz, S*C*PS$_2$), 151.70 (Tp^{Me2}), 151.28 (Tp^{Me2}), 150.69 (Tp^{Me2}), 150.66 (Tp^{Me2}), 150.08 (Tp^{Me2}), 147.16 (Tp^{Me2}), 146.76 (Tp^{Me2}), 146.16 (Tp^{Me2}), 145.42 (Tp^{Me2}), 144.32 (Tp^{Me2}), 106.82 (4-*C*-Tp^{Me2}), 106.68 (4-*C*-Tp^{Me2}), 106.58 (4-*C*-Tp^{Me2}), 106.45 (4-*C*-Tp^{Me2}), 106.37 (4-*C*-Tp^{Me2}), 106.27 (4-*C*-Tp^{Me2}), 68.02 (*THF*), 41.11 (d, $^1J_{PC}$ = 44.71 Hz, SiCH$_2$P), 32.69 (d, $^1J_{PC}$ = 34.45 Hz, SiCH$_2$P), 26.17 (*THF*), 16.52 (*C*H$_3$-Tp^{Me2}), 16.15 (*C*H$_3$-Tp^{Me2}), 15.58 (*C*H$_3$-Tp^{Me2}), 15.50 (*C*H$_3$-Tp^{Me2}), 14.49 (*C*H$_3$-Tp^{Me2}), 14.36 (*C*H$_3$-Tp^{Me2}), 13.18 (*C*H$_3$-Tp^{Me2}), 13.09 (*C*H$_3$-Tp^{Me2}), 13.04 (*C*H$_3$-Tp^{Me2}), 12.93 (*C*H$_3$-Tp^{Me2}), 12.85 (*C*H$_3$-Tp^{Me2}), 12.77 (*C*H$_3$-Tp^{Me2}), 9.27 (d, $^3J_{PC}$ = 7.28 Hz, Si(*C*H$_3$)$_2$), 8.66 (d, $^3J_{PC}$ = 11.6 Hz, Si(*C*H$_3$)$_2$), 6.41 (Si(*C*H$_3$)$_2$), 6.38 (Si(*C*H$_3$)$_3$), 6.25 (Si(*C*H$_3$)$_2$), 4.76 (Si(*C*H$_3$)$_3$); ^{31}P NMR (161 MHz, THF-d_8, 25 °C): δ (ppm) 92.43 (q, $^1J_{YP}$ = 17.6 Hz), 47.88 (s). Elemental analysis: calcd (%) for $C_{48}H_{86}N_{14}B_2OSi_4P_2S_4Y_2$: C, 41.86; H, 6.29; N, 14.24. Found: C, 41.14; H, 6.16; N, 14.45.

Synthesis of 4

A THF solution (10 mL) of **2** (230 mg, 0.20 mmol) was degassed using freeze–pump–thaw cycles and then exposed to an excess of 1.0 atm of CO. The color of the reaction mixture gradually changed from yellow to orange. After stirring at 50 °C for two days, the solvent was removed under vacuum to give an orange solid. The residue was washed twice with hexane (5 mL × 2) and dried under vacuum, giving **4** as an orange powder (185 mg, 74% yield). The orange single crystals of **4** for X-ray diffraction analysis were obtained by solvent evaporation from a concentrated toluene solution (*ca.* 2 mL) of **4**. ^{1}H NMR (400 MHz, toluene-d_8, 25 °C): δ (ppm) 5.61 (s, 2H, 4-*H*-Tp^{Me2}), 5.57 (s, 1H, 4-*H*-Tp^{Me2}), 5.50 (s, 2H, 4-*H*-Tp^{Me2}), 5.46 (s, 1H, 4-*H*-Tp^{Me2}), 3.67 (s, 4H, *THF*), 3.01 (s, 3H, CH_3-Tp^{Me2}), 2.93 (s, 3H, CH_3-Tp^{Me2}), 2.75 (s, 3H, CH_3-Tp^{Me2}), 2.64 (s, 3H, CH_3-Tp^{Me2}), 2.51 (s, 3H, CH_3-Tp^{Me2}), 2.43 (s, 3H, CH_3-Tp^{Me2}), 2.15–2.21 (m, 15H, CH_3-Tp^{Me2}), 2.06 (s, 3H, CH_3-Tp^{Me2}), 1.29–1.37 (m, 2H, SiCH_2P), 1.33 (s, 4H, *THF*), 1.08–1.22 (m, 4H, SiCH_2P), 0.66 (s, 3H, Si(CH_3)$_2$), 0.49 (s, 3H, Si(CH_3)$_2$), 0.41 (s, 6H, Si(CH_3)$_2$), −0.18 (s, 9H, Si(CH_3)$_3$), −0.22 (s, 9H, Si(CH_3)$_3$); ^{31}P NMR (161 MHz, toluene-d_8, 25 °C): δ (ppm) 65.01 (d, $^1J_{YP}$ = 136.4 Hz), −11.89 (d, $^1J_{YP}$ = 120.3 Hz). ^{1}H NMR (400 MHz, C_6D_6, 25 °C): δ (ppm) 5.64 (s, 3H, 4-*H*-Tp^{Me2}), 5.53 (s, 2H, 4-*H*-Tp^{Me2}), 5.46 (s, 1H, 4-*H*-Tp^{Me2}), 3.78 (m, 4H, *THF*), 3.15 (s, 3H, CH_3-Tp^{Me2}), 2.96 (s, 3H, CH_3-Tp^{Me2}), 2.81 (s, 3H, CH_3-Tp^{Me2}), 2.67 (s, 3H, CH_3-Tp^{Me2}), 2.56 (s, 3H, CH_3-Tp^{Me2}), 2.49 (s, 3H, CH_3-Tp^{Me2}), 2.11–2.21 (m, 15H, CH_3-Tp^{Me2}), 2.05

(s, 3H, CH_3-Tp^{Me2}), 1.29–1.37 (m, 2H, SiCH_2P), 1.17 (m, 2 + 4H, SiCH_2P + *THF*), 0.74 (s, 3H, Si(CH_3)$_2$), 0.57 (s, 3H, Si(CH_3)$_2$), 0.45 (s, 6H, Si(CH_3)$_2$), −0.09 (s, 9H, Si(CH_3)$_3$), −0.13 (s, 9H, Si(CH_3)$_3$); ^{13}C NMR (100 MHz, C_6D_6, 25 °C): δ (ppm) 151.55 (*C*O), 151.42 (Tp^{Me2}), 150.31 (Tp^{Me2}), 150.22 (Tp^{Me2}), 150.10 (Tp^{Me2}), 149.65 (Tp^{Me2}), 146.79 (Tp^{Me2}), 146.24 (Tp^{Me2}), 145.79 (Tp^{Me2}), 144.71 (Tp^{Me2}), 144.54 (Tp^{Me2}), 106.64 (4-*C*-Tp^{Me2}), 106.40 (4-*C*-Tp^{Me2}), 106.09 (4-*C*-Tp^{Me2}), 105.86 (4-*C*-Tp^{Me2}), 72.51 (*THF*), 25.14 (*THF*), 19.72 (d, $^1J_{PC}$ = 49.66 Hz, Si*C*H$_2$P), 15.84 (d, $^1J_{PC}$ = 12.42 Hz, Si*C*H$_2$P), 15.47 (CH_3-Tp^{Me2}), 15.33 (CH_3-Tp^{Me2}), 15.25 (CH_3-Tp^{Me2}), 15.07 (CH_3-Tp^{Me2}), 14.84 (CH_3-Tp^{Me2}), 14.71 (CH_3-Tp^{Me2}), 14.62 (CH_3-Tp^{Me2}), 13.21 (CH_3-Tp^{Me2}), 13.04 (CH_3-Tp^{Me2}), 12.98 (CH_3-Tp^{Me2}), 9.00 (Si(*C*H$_3$)$_2$), 8.44 (s, Si(*C*H$_3$)$_2$), 8.24 (s, Si(*C*H$_3$)$_2$), 5.81 (Si(*C*H$_3$)$_3$), 4.80 (Si(*C*H$_3$)$_3$), 1.43 (Si(*C*H$_3$)$_2$); ^{31}P NMR (161 MHz, C_6D_6, 25 °C): δ (ppm) 66.56 (br s), −11.81 (br s). Elemental analysis: calcd (%) for $C_{47}H_{86}N_{14}B_2O_2Si_4P_2Y_2$: C, 45.05; H, 6.92; N, 15.65. Found: C, 44.33; H, 6.77; N, 15.75.

Synthesis of 5

A cooled THF solution (3 mL) of PhNCS (27.5 mg, 0.20 mmol) was added slowly to a stirred THF solution (10 mL) of **2** (115.2 mg, 0.10 mmol) at ambient temperature. After stirring for 5 min, the reaction solution was left at room temperature for 2 days to give **5** as colorless crystals (145 mg, 93% yield). Regrettably, the low solubility of **5** precluded the acquisition of its NMR spectra. Elemental analysis: calcd (%) for $C_{64}H_{102}N_{16}B_2O_2Si_4P_2S_2Y_2$: C, 49.10; H, 6.57; N, 14.32. Found: C, 49.74; H, 6.52; N, 14.59.

Synthesis of 6 and 7

A cooled THF solution (5 mL) of PhNCO (47.6 mg, 0.40 mmol) was added slowly to a stirred THF solution (10 mL) of **2** (230 mg, 0.20 mmol) at ambient temperature. The color of the reaction solution gradually changed from yellow to colorless. After stirring at ambient temperature for 12 h, the solution was concentrated to *ca.* 3 mL under reduced pressure. After allowing to stand at room temperature for several days, colorless crystals of complex **6** were obtained (169 mg, 55% yield). However, if the reaction mixture was directly evaporated to dryness under vacuum, washing the residue with hexane three times (10 mL × 3) followed by crystallization in THF/hexane would lead to the loss of one coordinated THF, affording **7** as a crystalline solid (267 mg, 87% yield). Crystals suitable for X-ray diffraction analysis were obtained by gas phase diffusion of hexane into the THF solution of **7**. Notably, retransformation of **7** into **6** is quite difficult to perform in THF at room temperature, whereas transformation of **6** into **7** occurred slowly under vacuum conditions or exposure to nitrogen gas too. For example, the ^{31}P NMR monitoring data indicate the formation of a small amount of **7** after storing the solution of **6** in THF-d_8 at room temperature for 1 week (Fig. S14†). Therefore, compound **6** is not characterized by EA and NMR spectra. For **7**: ^{1}H NMR (400 MHz, THF-d_8, 25 °C): δ (ppm) 7.32 (d, 2H, $^3J_{HH}$ = 7.72 Hz, *Ph*), 7.03 (t, 2H, $^3J_{HH}$ = 7.32 Hz, *Ph*), 6.73 (t, 1H, $^3J_{HH}$ = 7.2 Hz, *Ph*), 6.27 (t, 1H, $^3J_{HH}$ = 7.08 Hz, *Ph*), 5.91 (m, 2H, *Ph*), 5.89 (s, 1H, 4-*H*-Tp^{Me2}), 5.82 (s, 1H, 4-*H*-Tp^{Me2}), 5.74 (s, 1H, 4-*H*-Tp^{Me2}), 5.59 (m, 2H, *Ph*), 5.54 (s, 1H, 4-*H*-Tp^{Me2}), 5.27 (s, 1H, 4-*H*-Tp^{Me2}), 5.27 (s, 1H, 4-*H*-Tp^{Me2}), 3.62 (m, 4H, *THF*), 2.57 (s, 6H, CH_3-Tp^{Me2}), 2.49 (s, 3H, CH_3-Tp^{Me2}), 2.45 (s, 3H, CH_3-Tp^{Me2}), 2.35 (s, 12H, CH_3-Tp^{Me2}), 2.31 (s, 3H, CH_3-Tp^{Me2}), 2.24 (s, 3H, CH_3-Tp^{Me2}), 2.04 (s, 3H, CH_3-Tp^{Me2}), 1.89–1.86 (m, 2H, SiCH_2P), 1.77 (m, 4H, *THF*), 1.61–1.54 (m, 2H, SiCH_2P), 1.47 (s, 3H, CH_3-Tp^{Me2}), 0.46 (s, 3H, Si(CH_3)$_2$), 0.44 (s, 3H, Si(CH_3)$_2$), 0.36 (s, 3H, Si(CH_3)$_2$), 0.21 (s, 3H, Si(CH_3)$_2$), −0.45 (s, 9H, Si(CH_3)$_3$), −0.67 (s, 9H, Si(CH_3)$_3$); ^{13}C {^{1}H} NMR (100 MHz, THF-d_8, 25 °C): δ (ppm) 181.61 (t, $^1J_{PC}$ = 5.0 Hz, P*C*=O), 165.83 (q, $^1J_{PC}$ = 3.0 Hz, P*C*=N), 151.38 (Tp^{Me2}), 150.44 (Tp^{Me2}), 150.42 (Tp^{Me2}), 149.96 (Tp^{Me2}), 149.69 (Tp^{Me2}), 149.54 (Tp^{Me2}), 146.34 (Tp^{Me2}), 146.04 (Tp^{Me2}), 144.88 (Tp^{Me2}), 144.49 (Tp^{Me2}), 128.11 (*Ph*), 127.44 (*Ph*), 126.72 (*Ph*), 125.34 (*Ph*), 124.84 (*Ph*), 123.61 (*Ph*), 122.27 (*Ph*), 121.01 (*Ph*), 106.71 (4-*C*-Tp^{Me2}), 106.48 (4-*C*-Tp^{Me2}), 106.24 (4-*C*-Tp^{Me2}), 105.82 (4-*C*-Tp^{Me2}), 105.20 (4-*C*-Tp^{Me2}), 104.74 (4-*C*-Tp^{Me2}), 68.02 (*THF*), 26.16 (*THF*), 15.43 (*C*H$_3$-Tp^{Me2}), 15.39 (*C*H$_3$-Tp^{Me2}), 15.06 (*C*H$_3$-Tp^{Me2}), 14.96 (*C*H$_3$-Tp^{Me2}), 14.33 (*C*H$_3$-Tp^{Me2}), 14.13 (*C*H$_3$-Tp^{Me2}), 14.06 (d, $^1J_{PC}$ = 27.45 Hz, Si*C*H$_2$P), 13.06 (d, $^1J_{PC}$ = 4.23 Hz, Si*C*H$_2$P), 12.93 (*C*H$_3$-Tp^{Me2}), 12.91 (*C*H$_3$-Tp^{Me2}), 12.87 (*C*H$_3$-Tp^{Me2}), 12.69 (*C*H$_3$-Tp^{Me2}), 9.64 (d, $^3J_{PC}$ = 5.09 Hz, Si(*C*H$_3$)$_2$), 7.59 (d, $^3J_{PC}$ = 10.91 Hz, Si(*C*H$_3$)$_2$), 6.31 (Si(*C*H$_3$)$_3$), 6.17 (Si(*C*H$_3$)$_2$), 4.68 (Si(*C*H$_3$)$_3$), 3.81 (d, $^3J_{PC}$ = 4.28 Hz, Si(*C*H$_3$)$_2$); ^{31}P NMR (161 MHz, THF-d_8, 25 °C): δ (ppm) −26.71 (dm, $^1J_{PP}$ = 374 Hz, PY), −39.64 (dd, J_{PP} = 374, 12.8 Hz, free P). Elemental analysis: calcd (%) for $C_{60}H_{94}N_{16}B_2O_3Si_4P_2Y_2$: C, 49.32; H, 6.48; N, 15.34. Found: C, 49.59; H, 6.34; N, 15.57.

Synthesis of 8

A THF solution (5 mL) of PhNNPh (39.6 mg, 0.20 mmol) was added slowly to a stirred THF solution (10 mL) of **2** (115 mg, 0.10 mmol) at ambient temperature. The colour of the reaction mixture gradually changed from yellow to greenish black. After stirring for 2 days, the solvent was removed under vacuum and the solid residue was washed twice with *n*-hexane (5 mL × 2) and dried under vacuum to give a yellow powder of **8** (141 mg, 85% yield). Yellow crystals suitable for X-ray diffraction analysis were obtained by solvent evaporation from a concentrated THF solution (*ca.* 2 mL) of 8. No satisfied ^{13}C NMR data of **8** were obtained due to its poor solubility. ^{1}H NMR (400 MHz, THF-d_8, 25 °C): δ (ppm) 7.31 (d, 4H, $^3J_{HH}$ = 7.92 Hz, –C$_6H_5$), 6.97 (t, $^3J_{HH}$ = 7.88 Hz, 6H, –C$_6H_5$), 6.70 (br, 2H, –C$_6H_5$), 6.63 (t, $^3J_{HH}$ = 7.12 Hz, 2H, –C$_6H_5$), 6.30 (br, 2H, –C$_6H_5$), 6.13 (t, $^3J_{HH}$ = 6.4 Hz, 4H, –C$_6H_5$), 5.87 (s, 2H, 4-*H*-Tp^{Me2}), 5.82 (s, 2H, 4-*H*-Tp^{Me2}), 5.60 (s, 2H, 4-*H*-Tp^{Me2}), 3.60 (m, 4H, *THF*), 2.64 (s, 6H, CH_3-Tp^{Me2}), 2.52 (s, 6H, CH_3-Tp^{Me2}), 2.48 (s, 6H, CH_3-Tp^{Me2}), 2.46 (s, 6H, CH_3-Tp^{Me2}), 2.45 (s, 6H, CH_3-Tp^{Me2}), 2.39–2.41 (m, 4H, SiCH_2P), 2.11 (s, 6H, CH_3-Tp^{Me2}), 1.77 (m, 4H, *THF*), 0.14 (s, 6H, Si(CH_3)$_2$), −0.38 (s, 18H, Si(CH_3)$_3$), −0.56 (s, 6H, Si(CH_3)$_2$); ^{31}P NMR (161 MHz, THF-d_8, 25 °C): δ (ppm) 50.66 (s). Elemental analysis: calcd (%) for $C_{74}H_{112}N_{18}B_2O_2Si_4P_2Y_2$: C, 53.56; H, 6.80; N, 15.19. Found: C, 53.27; H, 6.73; N, 15.27.

Synthesis of 9

A THF solution (5 mL) of S_8 (12.8 mg, 0.050 mmol) was added slowly to a stirred THF solution (10 mL) of **2** (115 mg, 0.10 mmol) at ambient temperature. After stirring for 5 min, the reaction solution was allowed to stand at room temperature for three days to give **9** as colorless crystals (120 mg, 94% yield). No satisfied NMR data of **9** were obtained due to its poor solubility even in heating THF-d_8. Elemental analysis: calcd (%) for $C_{42}H_{78}N_{14}B_2S_4Si_4P_2Y_2$: C, 39.37; H, 6.14; N, 15.31. Found: C, 38.53; H, 6.03; N, 15.26.

Synthesis of 10

Se powder (23.7 mg, 0.30 mmol) was added to a stirred THF solution (10 mL) of **2** (230 mg, 0.20 mmol) at ambient temperature. The color of the mixture gradually changed from greenish black to colorless. After stirring overnight and removing the solvent, a colorless solid was obtained, which was washed twice with hexane (10 mL × 2) and dried under vacuum to give **10** as a colorless powder (243 mg, 83% yield). Colorless crystals suitable for X-ray diffraction analysis were obtained by gas-phase diffusion of hexane into a concentrated THF solution (*ca.* 2 mL) of 10. ^{1}H NMR (400 MHz, THF-d_8, 25 °C): δ (ppm) 5.86 (s, 1H, 4-*H*-Tp^{Me2}), 5.83 (s, 3H, 4-*H*-Tp^{Me2}), 5.71 (s, 1H, 4-*H*-Tp^{Me2}), 5.60 (s, 1H, 4-*H*-Tp^{Me2}), 3.61 (m, 4H, *THF*), 2.75 (s, 3H, CH_3-Tp^{Me2}), 2.63 (s, 6H, CH_3-Tp^{Me2}), 2.60 (s, 3H, CH_3-Tp^{Me2}), 2.50 (s, 3H, CH_3-Tp^{Me2}), 2.44 (s, 12H, CH_3-Tp^{Me2}), 2.42 (s, 3H, CH_3-Tp^{Me2}), 2.34 (s, 3H, CH_3-Tp^{Me2}), 2.30 (s, 3H, CH_3-Tp^{Me2}), 2.12–2.27 (m, 4H, SiCH_2P), 1.77 (m, 4H, *THF*), 1.47 (s, 3H, CH_3-Tp^{Me2}), 0.42 (s, 3H, Si(CH_3)$_2$), 0.32 (s, 3H, Si(CH_3)$_2$), 0.30 (s, 6H, Si(CH_3)$_2$), −0.40 (s, 9H, Si(CH_3)$_3$), −0.50 (s, 9H, Si(CH_3)$_3$); ^{13}C NMR (100 MHz, THF-d_8, 25 °C): δ (ppm) 151.65 (Tp^{Me2}), 151.50 (Tp^{Me2}), 151.35 (Tp^{Me2}), 151.05 (Tp^{Me2}), 150.95 (Tp^{Me2}), 150.14 (Tp^{Me2}), 147.03 (Tp^{Me2}), 146.97 (Tp^{Me2}), 146.95 (Tp^{Me2}), 146.47 (Tp^{Me2}), 145.60 (Tp^{Me2}), 144.60 (Tp^{Me2}), 106.90 (4-*C*-Tp^{Me2}), 106.84 (4-*C*-Tp^{Me2}), 106.73 (4-*C*-Tp^{Me2}), 106.66 (4-*C*-Tp^{Me2}), 106.17 (4-*C*-Tp^{Me2}), 68.02 (*THF*), 34.68 (d, $^1J_{PC}$ = 5.34 Hz, Si*C*H$_2$P), 34.49 (d, $^1J_{PC}$ = 5.87 Hz, Si*C*H$_2$P), 26.16 (*THF*), 17.51 (CH_3-Tp^{Me2}), 17.28 (CH_3-Tp^{Me2}), 16.76 (CH_3-Tp^{Me2}), 15.59 (CH_3-Tp^{Me2}), 15.48 (CH_3-Tp^{Me2}), 14.77 (CH_3-Tp^{Me2}), 12.97 (CH_3-Tp^{Me2}), 12.89 (CH_3-Tp^{Me2}), 12.86 (CH_3-Tp^{Me2}), 7.54 (d, $^3J_{PC}$ = 3.81 Hz, Si(*C*H$_3$)$_2$), 7.46 (overlap d, Si(*C*H$_3$)$_2$), 7.42 (d, $^3J_{PC}$ = 3.65 Hz, Si(*C*H$_3$)$_2$), 6.80 (d, $^3J_{PC}$ = 5.19 Hz, Si(*C*H$_3$)$_2$), 5.53 (Si(*C*H$_3$)$_3$), 4.98 (s, Si(*C*H$_3$)$_3$); ^{31}P NMR (161 MHz, THF-d_8, 25 °C): δ (ppm) 29.97 (d, $^1J_{PP}$ = 390 Hz), 23.68 (d, $^1J_{PP}$ = 390 Hz). Elemental analysis: calcd (%) for $C_{46}H_{86}N_{14}B_2OSe_3Si_4P_2Y_2$: C, 37.79; H, 5.93; N, 13.41. Found: C, 37.53; H, 5.81; N, 13.29.

X-ray crystallographic analysis method

Suitable crystals were wrapped in mineral oil and then were frozen at 173 or 223 K. Data collections were performed on a Bruker SMART APEX (at 293 K) or Bruker SMART APEX (II) (at 173 or 293 K) diffractometer with a CCD area detector using graphite-monochromated Mo Kα radiation (λ = 0.71073 Å). Diffraction data were collected over the full sphere and corrected for absorption. Structure solutions were found with the SHELXS[42] package using direct methods and were refined with the SHELXTL program[43] against F^2 using first isotropic and late anisotropic thermal parameters for all non-hydrogen atoms. Hydrogen atoms were placed at calculated positions and included in the structure calculation without further refinement of the parameters. The residual electron densities were of no chemical significance. Details of SQUEEZE are given in the cif files. Unfortunately, the precision of compounds **5** and **6** was limited by the poor quality of their crystals.

Conclusions

In summary, we have developed a simple and effective method for the direct preparation of an amido-functionalized diphosphanato metal complex from P_4 and the corresponding silyl-bridged amido/methylene yttrium complex. Moreover, it is found that the resulting diphosphanato yttrium complex displays some distinctive reactivities unprecedented in diphosphine chemistry, such as redox metathesis/cyclization of the P_2 unit with CS_2, and multichalcogenylations of the P_2 unit with S_8 and Se without the P–P bond cleavage, which provide access to previously unattainable but potentially useful classes of new polyfunctional diphosphine-based ligands in a convenient metal-coordinated form. The results presented here not only demonstrate that appending a strongly coordinative substituent to the alkyl ligand together with a coordination to rare earth ions is an efficient strategy for controlling the alkylated cleavage modes of P_4, but also highlight the potential of the diphosphanato yttrium complex as a versatile P_2 synthon in the development of new polyfunctional diphosphine ligands, achieved by the controllable Y–P and P–P bond insertions, P-based oxidation or their combination with other types of reactions. This valuable discovery opens up new pathways for the construction of cyclic and acyclic polyfunctional diphosphorus-containing organic ligands from white phosphorus and inexpensive, relatively simple and readily available small molecule substrates with perfect atom economy. This valuable discovery makes a previously unattainable class of dppm-like ligands, with varied substituents on the phosphorus donors, readily available, even those thought to be inaccessible due to the instability of the free diphosphinothioether. More research is currently underway to explore the chemistry of this underutilized class of polyfunctional diphosphine-based ligands.

Author contributions

All authors have given approval to the final version of the manuscript. F. Z. and K. H. synthesized and analyzed all new compounds. J. Z. conceived the idea and supervised the work. J. Z. and X. Z. interpreted the results. I. R. and L. M. conducted DFT calculations. All authors contributed to the preparation of the manuscript.

Conflicts of interest

There are no conflicts to declare.

Acknowledgements

This work was supported by the National Natural Science Foundation of China (grant no. 21871058, 22271051, and 22371049) and the 973 program (2015CB856600). LM is a member of the Institut Universitaire de France. Fudan University and the Chinese Academy of Science are acknowledged for financial support through visiting grants (LM). The authors also acknowledge the HPCs CALcul en Midi-Pyrénées (CALMIP-EOS grant 1415). We also greatly acknowledge Dr Yuejian Lin for single crystal X-ray diffraction analysis.

References

1 For reviews on the application of diphosphines in catalysis, see: (*a*) W. Tang and X. Zhang, New Chiral Phosphorus Ligands for Enantioselective Hydrogenation, *Chem. Rev.*, 2003, **103**, 3029; (*b*) M. Berthod, G. Mignani, G. Woodward and M. Lemaire, Modified BINAP: The How and the Why, *Chem. Rev.*, 2005, **105**, 1801; (*c*) Y.-M. Li, F.-Y. Kwong, W.-Y. Yu and A. S. C. Chan, Recent Advances in Developing New Axially Chiral Phosphine Ligands for Asymmetric Catalysis, *Coord. Chem. Rev.*, 2007, **251**, 2119.

2 For reviews on metal complexes bearing diphosphine ligands, see: (*a*) B. Chaudret, B. Delavaux and R. Poilblanc, Bisdiphenylphosphinomethane in Dinuclear Complexes, *Coord. Chem. Rev.*, 1988, **86**, 191; (*b*) C. A. Besse, P. Aggarwal, A. C. Marschilok and K. J. Takeuchi, Transition-Metal Complexes Containing Trans-Spanning Diphosphine Ligands, *Chem. Rev.*, 2001, **101**, 1031; (*c*) M. Knorr and I. Jourdain, Activation of Alkynes by Diphosphine- and μ-Phosphido-Spanned Heterobimetallic Complexes, *Coord. Chem. Rev.*, 2017, **350**, 217.

3 (*a*) S. L. James, Phosphines as Building Blocks in Coordination-Based Self-Assembly, *Chem. Soc. Rev.*, 2009, **38**, 1744; (*b*) K. Konishi, M. Iwasaki and Y. Shichibu, Phosphine-Ligated Gold Clusters with Core+exo Geometries: Unique Properties and Interactions at the Ligand–Cluster Interface, *Acc. Chem. Res.*, 2018, **51**, 3125.

4 (*a*) M. Driess, A. D. Fantu, D. R. Powell and R. West, Synthesis, Characterization, and Complexation of an Unusual P2Si2 Bicyclobutane with Butterfly-Structure: 2,2,4,4-Tetramesityl-1,3-diphospha-2,4-disilabicyclo[1.1.0] butane, *Angew. Chem., Int. Ed. Engl.*, 1989, **28**, 1038; (*b*) J.-C. Hierso, R. Smaliy, R. Amardeil and P. Meunier, New Concepts in Multidentate Ligand Chemistry: Effects of multidentarity on Catalytic and Spectroscopic Properties of Ferrocenyl Polyphosphines, *Chem. Soc. Rev.*, 2007, **36**, 1754; (*c*) M.-N. Birkholz, Z. Freixab and P. W. N. M. van Leeuwen, Bite Angle Effects of Diphosphines in C–C and C–X Bond Forming Cross Coupling Reactions, *Chem. Soc. Rev.*, 2009, **38**, 1099; (*d*) M. Zablocka, A. Hameau, A.-M. Caminade and J.-P. Majoral, "Cage-Like" Phosphines: Design and Catalytic Properties, *Adv. Synth. Catal.*, 2010, **352**, 2341; (*e*) S. S. Sen, S. Khan, H. W. Roesky, D. Kratzert, K. Meindl, J. Henn, D. Stalke, J.-P. Demers and A. Lange, Zwitterionic Si-C-Si-P and Si-P-Si-P Four-Membered Rings with Two-Coordinate Phosphorus Atoms, *Angew. Chem., Int. Ed.*, 2011, **50**, 2322.

5 (*a*) N. A. Piro, J. S. Figueroa, J. T. McKellar and C. C. Cummins, Triple-Bond Reactivity of Diphosphorus Molecules, *Science*, 2006, **313**, 1276; (*b*) A. Velian and C. C. Cummins, Synthesis and Characterization of P2N3−: An Aromatic Ion Composed of Phosphorus and Nitrogen, *Science*, 2015, **348**, 1001; (*c*) C. Hering-Junghans and E. Rivard, Accessing an Aromatic Diphosphatriazolate Anion by Formal Inorganic "Click" Chemistry, *Angew. Chem., Int. Ed.*, 2015, **54**, 10077; (*d*) K. Helmdach, S. Ludwig, A. Villinger, D. Hollmann, J. Kösters and W. W. Seidel, Synthesis and Activation Potential of an Open Shell Diphosphine, *Chem. Commun.*, 2017, **53**, 5894; (*e*) A. J. Arggelles, S. Sun, B. G. Budaitis and P. Nagorny, Design, Synthesis, and Application of Chiral C2-Symmetric Spiroketal-Containing Ligands in Transition-Metal Catalysis, *Angew. Chem., Int. Ed.*, 2018, **57**, 5325.

6 (*a*) O. Back, G. Kuchenbeiser, B. Donnadieu and G. Bertrand, Nonmetal-Mediated Fragmentation of P4: Isolation of P1 and P2 Bis(carbene) Adducts, *Angew. Chem., Int. Ed.*, 2009, **48**, 5530; (*b*) D. Tofan and C. C. Cummins, Photochemical Incorporation of Diphosphorus Units into Organic Molecules, *Angew. Chem., Int. Ed.*, 2010, **49**, 7516; (*c*) O. Back, B. Donnadieu, P. Parameswaran, G. Frenking and G. Bertrand, Isolation of Crystalline Carbene-Stabilized P2-Radical Cations and P2-Dications, *Nat. Chem.*, 2010, **2**, 369; (*d*) I. Knopf, D. Tofan, D. Beetstra, A. Al-Nezari, K. Al-Bahily and C. C. Cummins, A Family of cis-Macrocyclic Diphosphines: Modular, Stereoselective Synthesis and Application in Catalytic CO2/Ethylene Coupling, *Chem. Sci.*, 2017, **8**, 1463.

7 (*a*) H. Shimizu, I. Nagasaki, K. Matsumura, N. Sayo and T. Saito, Developments in Asymmetric Hydrogenation from an Industrial Perspective, *Acc. Chem. Res.*, 2007, **40**, 1385; (*b*) J.-H. Xie, S.-F. Zhu and Q.-L. Zhou, Recent Advances in Transition Metal-Catalyzed Enantioselective Hydrogenation of Unprotected Enamines, *Chem. Soc. Rev.*, 2012, **41**, 4126; (*c*) J. Barwick-Silk, S. Hardy, M. C. Willis and A. S. Weller, Rh(DPEPhos)-Catalyzed Alkyne Hydroacylation Using β-Carbonyl-Substituted Aldehydes: Mechanistic Insight Leads to Low Catalyst Loadings that Enables Selective Catalysis on Gram-Scale, *J. Am. Chem. Soc.*, 2018, **140**, 7347.

8 J. R. Dilworth and N. Wheatley, The Preparation and Coordination Chemistry of Phosphorus Sulfur Donor Ligands, *Coord. Chem. Rev.*, 2000, **199**, 89.

9 (*a*) L.-C. Liang, Metal Complexes of Chelating Diarylamido Phosphine Ligands, *Coord. Chem. Rev.*, 2006, **250**, 1152; (*b*) M. T. Whited and R. H. Grubbs, Late Metal Carbene Complexes Generated by Multiple C–H Activations:

Examining the Continuum of M=C Bond Reactivity, *Acc. Chem. Res.*, 2009, **42**, 1607; (*c*) M. J. Sgro and D. W. Stephan, Frustrated Lewis Pair Inspired Carbon Dioxide Reduction by a Ruthenium Tris(aminophosphine) Complex, *Angew. Chem., Int. Ed.*, 2012, **51**, 11343; (*d*) R. M. Bullock and M. L. Helm, Molecular Electrocatalysts for Oxidation of Hydrogen Using Earth-Abundant Metals: Shoving Protons Around with Proton Relays, *Acc. Chem. Res.*, 2015, **48**, 2017; (*e*) P. Bhattacharya, D. E. Prokopchuk and M. T. Mock, Exploring the Role of Pendant amines in Transition Metal Complexes for the Reduction of N2 to Hydrazine and Ammonia, *Coord. Chem. Rev.*, 2017, **334**, 67.

10 J.-P. Genet, T. Ayad and V. Ratovelomanana-Vidal, Electron-Deficient Diphosphines: The Impact of DIFLUORPHOS in Asymmetric Catalysis, *Chem. Rev.*, 2014, **114**, 2824.

11 M. S. Balakrishna, P. Chandrasekaran and P. P. George, Silicon Based Phosphines with P-Si-P, P-C-Si-C-P and P-O-Si-O-P Linkages and Their Coordination Chemistry and Catalytic Applications, *Coord. Chem. Rev.*, 2003, **241**, 87.

12 Y. Zhang, M. Schulz, M. Wächtler, M. Karnahl and B. Dietzek, Heteroleptic Diimine–Diphosphine Cu(ı) Complexes as an Alternative towards Noble-Metal Based Photosensitizers: Design Strategies, Photophysical Properties and Perspective Applications, *Coord. Chem. Rev.*, 2018, **356**, 127.

13 (*a*) A. H. Cowley, D. M. Giolando, C. M. Nunn, M. Pakulski, D. Westmoreland and N. C. Norman, Synthesis and Reactivity of Mononuclear Molybdenum Phosphido Complexes, [Mo(CO)2{P(Cl)R}(η-C5H5)][R = CH(SiMe3)2 or NCMe2CH2CH2CH2CMe2]. X-Ray Crystal Structures of [Mo(CO)2{P(x)(NCMe2CH2CH2CH2CMe2)}(η-C5H5)](X = Cl or NMe2) and [Mo2(CO)4{μ-P2[CH(SiMe3)2]2}(η-C5H5)2], *J. Chem. Soc., Dalton Trans.*, 1988, 2127; (*b*) Y. Lv, C. E. Kefalidis, J. Zhou, L. Maron, X. Leng and Y. Chen, Versatile Reactivity of a Four-Coordinate Scandium Phosphinidene Complex: Reduction, Addition, and CO Activation Reactions, *J. Am. Chem. Soc.*, 2013, **135**, 14784.

14 (*a*) M. Scheer, G. Balázs and A. Seitz, P4 Activation by Main Group Elements and Compounds, *Chem. Rev.*, 2010, **110**, 4236; (*b*) B. M. Cossairt, N. A. Piro and C. C. Cummins, Early-Transition-Metal-Mediated Activation and Transformation of White Phosphorus, *Chem. Rev.*, 2010, **110**, 4164; (*c*) M. Caporali, L. Gonsalvi, A. Rossin and M. Peruzzini, P4 Activation by Late-Transition Metal Complexes, *Chem. Rev.*, 2010, **110**, 4178; (*d*) N. A. Giffin and J. D. Masuda, Reactivity of White Phosphorus with Compounds of the p-Block, *Coord. Chem. Rev.*, 2011, **255**, 1342.

15 N. Etkin, M. T. Benson, S. Courtenay, M. J. McGlinchey, A. D. Bain and D. W. Stephan, Niobium and Tantalum Diphosphanato Complexes: Synthesis, Structure, and NMR Studies of Cp2MH[(PR)2] (R = Ph, Cy, H), *Organometallics*, 1997, **16**, 3504.

16 (*a*) R. Riedel, H.-D. Hausen and E. Fluck, Bis(2,4,6-tri-tert-butylphenyl)bicyclotetraphosphane, *Angew. Chem., Int. Ed. Engl.*, 1985, **24**, 1056; (*b*) A. Hübner, T. Bernert, I. Sänger, E. Alig, M. Bolte, L. Fink, M. Wagner and H.-W. Lerner, Solvent-Free Mesityllithium: Solid-State Structure and Its Reactivity towards White Phosphorus, *Dalton Trans.*, 2010, **39**, 7528.

17 T. Arnold, H. Braunschweig, J. O. C. Jimenez-Halla, K. Radacki and S. S. Sen, Simultaneous Fragmentation and Activation of White Phosphorus, *Chem. – Eur. J.*, 2013, **19**, 9114.

18 (*a*) L. Xu, Y. Chi, S. Du, W.-X. Zhang and Z.-F. Xi, Direct Synthesis of Phospholyl Lithium from White Phosphorus, *Angew. Chem., Int. Ed.*, 2016, **55**, 9187; (*b*) S. K. Ghosh, C. C. Cummins and J. A. Gladysz, A Direct Route from White Phosphorus and Fluorous Alkyl and Aryl Iodides to the Corresponding Trialkyl- and Triarylphosphines, *Org. Chem. Front.*, 2018, **5**, 3421.

19 (*a*) A. R. Fox, R. J. Wright, E. Rivard and P. P. Power, Tl2[Aryl2P4]: A Thallium Complexed Diaryltetraphosphabutadienediide and its Two-Electron Oxidation to a Diaryltetraphosphabicyclobutane, Aryl2P4, *Angew. Chem., Int. Ed.*, 2005, **44**, 7729; (*b*) S. Heinl, S. Reisinger, C. Schwarzmaier, M. Bodensteiner and M. Scheer, Selective Functionalization of P4 by Metal-Mediated C-P Bond Formation, *Angew. Chem., Int. Ed.*, 2014, **53**, 7639; (*c*) J. E. Borger, A. W. Ehlers, M. Lutz, J. C. Slootweg and K. Lammertsma, Functionalization of P4 Using a Lewis Acid Stabilized Bicyclo[1.1.0]tetraphosphabutane Anion, *Angew. Chem., Int. Ed.*, 2014, **53**, 12836; (*d*) M. Arrowsmith, M. S. Hill, A. L. Johnson, G. Kociok-Köhn and M. F. Mahon, Attenuated Organomagnesium Activation of White Phosphorus, *Angew. Chem., Int. Ed.*, 2015, **54**, 7882; (*e*) J. E. Borger, A. W. Ehlers, M. Lutz, J. C. Slootweg and K. Lammertsma, Stabilization and Transfer of the Transient [Mes*P4]– Butterfly Anion Using BPh3, *Angew. Chem., Int. Ed.*, 2016, **55**, 613; (*f*) S. Du, J. Yin, Y. Chi, L. Xu and W.-X. Zhang, Dual Functionalization of White Phosphorus: Formation, Characterization, and Reactivity of Rare-Earth-Metal Cyclo-P3 Complexes, *Angew. Chem., Int. Ed.*, 2017, **56**, 15886.

20 (*a*) O. J. Scherer, M. Ehses and G. Wolmershäuser, Activation of P4 and P2 by Transition Metal Complexes at Room Temperature, *Angew. Chem., Int. Ed.*, 1998, **37**, 507; (*b*) J. S. Figueroa and C. C. Cummins, The Niobaziridine–Hydride Functional Group: Synthesis and Divergent Reactivity, *J. Am. Chem. Soc.*, 2003, **125**, 4020; (*c*) E. B. Hulley, P. T. Wolczanski and E. B. Lobkovsky, [(silox)3M]2(μ:η1,η1-P2) (M = Nb, Ta) and [(silox)3Nb]2{μ:η2,η2-(cP3–cP3)} from (silox)3M (M = NbPMe3, Ta) and P4 (silox = tBu3SiO), *Chem. Commun.*, 2009, 6412; (*d*) M. Demange, X.-F. Goff, P. L. Floch and N. Mézailles, P4 Activation with Pt0 Metal Centers: Selective Formation of a Dinuclear {Pt2(μ,η2:2-P2)} Complex, *Chem. – Eur. J.*, 2010, **16**, 12064.

21 (*a*) L. Weber, The Chemistry of Diphosphenes and Their Heavy Congeners: Synthesis, Structure, and Reactivity, *Chem. Rev.*, 1992, **92**, 1839; (*b*) J. Y. Hu, W. Liu and

W. X. Zhang, Direct functionalization of white phosphorus by organolithium reagents to organophosphorus compounds, *Phosphorus, Sulfur Silicon Relat. Elem.*, 2022, **197**(5–6), 398–407; (*c*) G. Luo, S. Du, P. Wang, F. Liu, W. X. Zhang and Y. Luo, Fragmentation Mechanism of White Phosphorus: A Theoretical Insight into Multiple Cleavage/Formation of P–P and P–C Bonds, *Chem. – Eur. J.*, 2020, **26**, 13282; (*d*) Z. J. Lv, Z. Huang, J. H. Shen, W. X. Zhang and Z. F. Xi, Well-Defined Scandacyclopropenes: Synthesis, Structure, and Reactivity, *J. Am. Chem. Soc.*, 2019, **141**, 20547.

22 (*a*) P. Coburger, S. Demeshko, C. Rödl, E. Hey-Hawkins and R. Wolf, Oxidative P-P-Bindungsaddition an Cobalt(−I): Bildung eines Low-spin-Cobalt(III)-Phosphanidokomplexes, *Angew. Chem., Int. Ed.*, 2017, **56**, 15871; (*b*) Y.-E. Kim and Y. Lee, A P–P Bond as a Redox Reservoir and an Active Reaction Site, *Angew. Chem., Int. Ed.*, 2018, **57**, 14159.

23 (*a*) H. Schäfer, D. Binder and D. Fenske, Chelate-Stabilized Diphosphene and Diphosphorus Complexes of Nickel, *Angew. Chem., Int. Ed. Engl.*, 1985, **24**, 522; (*b*) S. Xin, H. G. Woo, J. F. Harrod, E. Samuel and A.-M. Lebuis, Synthesis and Crystal Structure of Some Novel Titanocene Phosphido Compounds by P–H Activation in the Presence of Hydrosilanes, *J. Am. Chem. Soc.*, 1997, **119**, 5307; (*c*) P. M. Scheetz, D. S. Glueck and A. L. Rheingold, Rhodium-Catalyzed Isomerization of a Bis(secondary phosphine) to an Unsymmetrical Diphosphine via P–C Cleavage and P–P and C–H Bond Formation, *Organometallics*, 2017, **36**, 3387.

24 (*a*) J. Hong, H. Tian, L. Zhang, X. Zhou, I. Rosal, L. Weng and L. Maron, Reversing Conventional Reactivity of Mixed Oxo/Alkyl Rare-Earth Complexes: Non-Redox Oxygen Atom Transfer, *Angew. Chem., Int. Ed.*, 2018, **57**, 1062; (*b*) J. Zhou, L. Xiang, J. Guo, X. Leng and Y. Chen, Formation and Reactivity of a C-P-N-Sc Four-Membered Ring: H2, O2, CO, Phenylsilane, and Pinacolborane Activation, *Chem. – Eur. J.*, 2017, **23**, 5424; (*c*) V. Radkov, T. Roisnel, A. Trifonov, J.-F. Carpentier and E. Kirillov, Tandem C(sp2)–OMe Activation/C(sp2)–C(sp2) Coupling in Early Transition-Metal Complexes: Aromatic C–O Activation beyond Late Transition Metals, *J. Am. Chem. Soc.*, 2016, **138**, 4350; (*d*) M. E. Fieser, J. E. Bates, J. W. Ziller, F. Furche and W. J. Evans, Dinitrogen Reduction via Photochemical Activation of Heteroleptic Tris(cyclopentadienyl) Rare-Earth Complexes, *J. Am. Chem. Soc.*, 2013, **135**, 3804.

25 (*a*) J.-B. Zhu, E. M. Watson, J. Tang and E. Y.-X. Chen, A Synthetic Polymer System with Repeatable Chemical Recyclability, *Science*, 2018, **360**, 398; (*b*) Y. Shao, F. Zhang, J. Zhang and X. Zhou, Lanthanide-Catalyzed Reversible Alkynyl Exchange by Carbon–Carbon Single-Bond Cleavage Assisted by a Secondary Amino Group, *Angew. Chem., Int. Ed.*, 2016, **55**, 11485; (*c*) T. L. Lohr, Z. Li and T. J. Marks, Thermodynamic Strategies for C–O Bond Formation and Cleavage via Tandem Catalysis, *Acc. Chem. Res.*, 2016, **49**, 824; (*d*) M. Nishiura, F. Guo and Z. Hou, Half-Sandwich Rare-Earth-Catalyzed Olefin Polymerization, Carbometalation, and Hydroarylation, *Acc. Chem. Res.*, 2015, **48**, 2209.

26 (*a*) Q. You, J. Zhang, F. Zhang, J. Cai and X. Zhou, Cooperative Rare-Earth/Lithium-Mediated Conversion of White Phosphorus, *Chem. – Eur. J.*, 2023, e202203679; (*b*) F. Zhang, K. Han, J. Cai, Z. Ye, J. Zhang, X. Zhou and Z. Li, Rare-Earth-Mediated Conversion of White Phosphorus into PBn3 and Highly Functionalized Norbornane-P7, *Inorg. Chem. Front.*, 2024, **11**, 478–486; (*c*) F. Zhang, J. Zhang, Z. Chen, L. Weng and X. Zhou, An Yttrium Organic Cyclo-P4 Complex and Its Selective Conversions, *Inorg. Chem.*, 2019, **58**, 8451.

27 (*a*) J. Andrez, J. Pécaut, P.-A. Bayle and M. Mazzanti, Tuning Lanthanide Reactivity Towards Small Molecules with Electron-Rich Siloxide Ligands, *Angew. Chem., Int. Ed.*, 2014, **53**, 10448; (*b*) X.-F. Jiang, H. Huang, Y.-F. Chai, T. L. Lohr, S.-Y. Yu, W.-Z. Lai, Y.-J. Pan, M. Delferro and T. J. Marks, Hydrolytic Cleavage of Both CS2 Carbon–Sulfur Bonds by Multinuclear Pd(II) Complexes at Room Temperature, *Nat. Chem.*, 2017, **9**, 188.

28 (*a*) W. Petz, 40 Years of Transition-Metal Thiocarbonyl Chemistry and the Related CSe and CTe Compounds, *Coord. Chem. Rev.*, 2008, **252**, 1689; (*b*) L. Wang, W. He and Z. Yu, Transition-Metal Mediated Carbon–Sulfur Bond Activation and Transformations, *Chem. Soc. Rev.*, 2013, **42**, 599.

29 (*a*) H. Zhu, J. Chai, Q. Ma, V. Jancik, H. W. Roesky, H. Fan and R. Herbst-Irmer, A Seven-Membered Aluminum Sulfur Allenyl Heterocycle Arising from the Conversion of an Aluminacyclopropene with CS2, *J. Am. Chem. Soc.*, 2004, **126**, 10194; (*b*) J. Ballmann, A. Yeo, B. A. MacKay, S. V. Rijt, B. O. Patrick and M. D. Fryzuk, Complete Disassembly of Carbon Disulfide by a Ditantalum Complex, *Chem. Commun.*, 2010, **46**, 8794; (*c*) S. I. Kalläne, T. Braun, M. Teltewskoi, B. Braun, R. Herrmann and R. Laubenstein, Remarkable Reactivity of a Rhodium(I) Boryl Complex towards CO2 and CS2: Isolation of a Carbido Complex, *Chem. Commun.*, 2015, **51**, 14613; (*d*) M. Falcone, L. Chatelain and M. Mazzanti, Nucleophilic Reactivity of a Nitride-Bridged Diuranium(IV) Complex: CO2 and CS2 Functionalization, *Angew. Chem., Int. Ed.*, 2016, **55**, 4074.

30 (*a*) K. Wang, G. Luo, J. Hong, X. Zhou, L. Weng, Y. Luo and L. Zhang, Homometallic Rare-Earth Metal Phosphinidene Clusters: Synthesis and Reactivity, *Angew. Chem., Int. Ed.*, 2014, **53**, 1053; (*b*) F. Dielmann and G. Bertrand, Reactivity of a Stable Phosphinonitrene towards Small Molecules, *Chem. – Eur. J.*, 2015, **21**, 191; (*c*) H. Tian, J. Hong, K. Wang, I. Rosal, L. Maron, X. Zhou and L. Zhang, Unprecedented Reaction Mode of Phosphorus in Phosphinidene Rare-Earth Complexes: A Joint Experimental–Theoretical Study, *J. Am. Chem. Soc.*, 2018, **140**, 102.

31 H. Heuclin, X. F. Goff and N. Mézailles, Mixed (P=S/P=O)-Stabilized Geminal Dianion: Facile Diastereoselective Intramolecular C-H Activations by a Related Ruthenium–Carbene Complex, *Chem. – Eur. J.*, 2012, **18**, 16136.

32 (*a*) T. M. Trnka and R. H. Grubbs, The Development of L2X2Ru=CHR Olefin Metathesis Catalysts: An

Organometallic Success Story, *Acc. Chem. Res.*, 2001, **34**, 18; (*b*) I. Nakamura and Y. Yamamoto, Transition-Metal-Catalyzed Reactions in Heterocyclic Synthesis, *Chem. Rev.*, 2004, **104**, 2127; (*c*) S. Fustero, A. Simón-Fuentes, P. Barrio and G. Haufe, Olefin Metathesis Reactions with Fluorinated Substrates, Catalysts, and Solvents, *Chem. Rev.*, 2015, **115**, 871.

33 (*a*) J. R. Ludwig, P. M. Zimmerman, J. B. Gianino and C. S. Schindler, Iron(III)-Catalysed Carbonyl–Olefin Metathesis, *Nature*, 2016, **533**, 374; (*b*) M. A. Aljuhani, S. Barman, E. Abou-Hamad, A. Gurinov, S. Ould-Chikh, E. Guan, A. Jedidi, L. Cavallo, B. C. Gates, J. D. A. Pelletier and J.-M. Basset, Imine Metathesis Catalyzed by a Silica-Supported Hafnium Imido Complex, *ACS Catal.*, 2018, **8**, 9445.

34 R. J. Newland, J. M. Lynam and S. M. Mansell, Small Bite-Angle 2-Phosphinophosphinine Ligands Enable Rhodium-Catalysed Hydroboration of Carbonyls, *Chem. Commun.*, 2018, **54**, 5482.

35 (*a*) W. J. Evans, K. J. Forrestal and J. W. Ziller, Synthesis and Structure of a Thermally Stable, Nonclassical, 7-Norbornadienyl Carbocation Obtained from (C5Me5)3Sm and CO, *J. Am. Chem. Soc.*, 1995, **117**, 12635; (*b*) B. Wang, G. Luo, M. Nishiura, Y. Luo and Z. Hou, Cooperative Trimerization of Carbon Monoxide by Lithium and Samarium Boryls, *J. Am. Chem. Soc.*, 2017, **139**, 16967.

36 (*a*) W. J. Evans, D. S. Lee, J. W. Ziller and N. Kaltsoyannis, Trivalent [(C5Me5)2(THF)Ln]2(μ-η2:η2-N2) Complexes as Reducing Agents Including the Reductive Homologation of CO to a Ketene Carboxylate, (μ-η4-O2C-C=C=O)2−, *J. Am. Chem. Soc.*, 2006, **128**, 14176; (*b*) T. Shima and Z. Hou, Hydrogenation of Carbon Monoxide by Tetranuclear Rare Earth Metal Polyhydrido Complexes. Selective Formation of Ethylene and Isolation of Well-Defined Polyoxo Rare Earth Metal Clusters, *J. Am. Chem. Soc.*, 2006, **128**, 8124; (*c*) J. Cheng, M. J. Ferguson and J. Takats, Synthesis and Reaction of [(TpiPr2)LnH2]3 (Ln = Y, Lu) with CO: Trinuclear Cluster-Bound Propenolate en Route to Selective Formation of Propene, *J. Am. Chem. Soc.*, 2010, **132**, 2.

37 (*a*) M. H. Holthausen and J. J. Weigand, Preparation of the [(DippNP)2(P4)2]2+-Dication by the Reaction of [DippNPCl] 2 and a Lewis Acid with P4, *J. Am. Chem. Soc.*, 2009, **131**, 14210; (*b*) J. Cui, Y. Li, R. Ganguly, A. Inthirarajah, H. Hirao and R. Kinjo, Metal-Free σ-Bond Metathesis in Ammonia Activation by a Diazadiphosphapentalene, *J. Am. Chem. Soc.*, 2014, **136**, 16764.

38 (*a*) L.-X. Zhang, T. Suzuki, Y. Luo, M. Nishiura and Z. Hou, Cationic Alkyl Rare-Earth Metal Complexes Bearing an Ancillary Bis(phosphinophenyl)amido Ligand: A Catalytic System for Living cis-1,4-Polymerization and Copolymerization of Isoprene and Butadiene, *Angew. Chem., Int. Ed.*, 2007, **46**, 1909; (*b*) J. Bravo, C. Cativiela, J. E. Chaves, R. Navarro and E. P. Urriolabeitia, 31P NMR Spectroscopy as a Powerful Tool for the Determination of Enantiomeric Excess and Absolute Configurations of α-Amino Acids, *Inorg. Chem.*, 2003, **42**, 1006.

39 (*a*) D. Tofan, B. M. Cossairt and C. C. Cummins, White Phosphorus Activation at a Metal–Phosphorus Triple Bond: a New Route to cyclo-Triphosphorus or cyclo-Pentaphosphorus Complexes of Niobium, *Inorg. Chem.*, 2011, **50**, 12349; (*b*) D. Tofan, M. Temprado, S. Majumdar, C. D. Hoff and C. C. Cummins, Functionalization Reactions Characteristic of a Robust Bicyclic Diphosphane Framework, *Inorg. Chem.*, 2013, **52**, 8851.

40 P. Brunel, J. Monot, C. E. Kefalidis, L. Maron, B. Martin-Vaca and D. Bourissou, Valorization of CO2: Preparation of 2-Oxazolidinones by Metal–Ligand Cooperative Catalysis with SCS Indenediide Pd Complexes, *ACS Catal.*, 2017, **7**, 2652.

41 W. Yi, J. Zhang, F. Zhang, Y. Zhang, Z. Chen and X. Zhou, Versatile Reactivity of Scorpionate-Anchored Yttrium Dialkyl Complexes towards Unsaturated Substrates, *Chem. – Eur. J.*, 2013, **19**, 11975.

42 G. M. Sheldrick, A short history of SHELX, *Acta Crystallogr., Sect. A: Found. Crystallogr.*, 2008, **64**, 112.

43 G. M. Sheldrick, *SHELXL-2014, Program for Refinement of Crystal Structures*, University of Göttingen, Göttingen, Germany, 2014.